Environmental Science & Technology

pubs.acs.org/est

Article

Pseudomonas sp. Strain 273 Metabolizes Decanes with Poly- or Perfluorinated Carbons

Alexander S. Walls, Gao Chen, Diana Ramirez, Yongchao Xie, Broquell M. Wong, Amanda L. May, Anita Thapalia, Frank E. Löffler,* and Shawn R. Campagna*

Cite This: *Environ. Sci. Technol.* 2025, 59, 22663−22675

Read Online

ACCESS | Metrics & More | Article Recommendations | Supporting Information

ABSTRACT: During growth with terminally monofluorinated decanes, the soil isolate *Pseudomonas* sp. strain 273 releases inorganic fluoride and channels fluorometabolites into glycerophospholipid biosynthesis. We explored the ability of this bacterium to metabolize 1,1-difluorodecane (F2-decane), 1,1,1-trifluorodecane (F3-decane), and 1,1,1,2,2-pentafluorodecane (F5-decane) to assess the impacts of increasing degree of fluorination on organismal metabolism. Growth occurred with all three polyfluorodecane substrates, and inorganic fluoride release was observed in cultures amended with F2-decane and F5-decane but not with F3-decane. Fluorine nuclear magnetic resonance spectroscopy (^{19}F NMR) detected polyfluorinated C_6 and C_4 short-chain fatty acid catabolites suggesting incomplete β-oxidation during catabolism by strain 273. Gas chromatography−mass spectrometry (GC-MS) analysis corroborated the formation of terminally poly- or perfluorinated short-chain fatty acids. Ultrahigh performance liquid chromatography-high resolution mass spectrometry (UHPLC-HRMS) based global lipidome profiling revealed glycerophospholipids with fluorine substitutions at the sn1/sn2 acyl chains and identified a range of glycerophospholipids that contained between two and ten fluorines depending on the growth substrate. These findings advance our understanding of bacterial transformation of alkanes with poly- and perfluorinated carbons and highlight the formation of short-chain fluorinated fatty acids as catabloc products and fluorophospholipids as anabolic products.

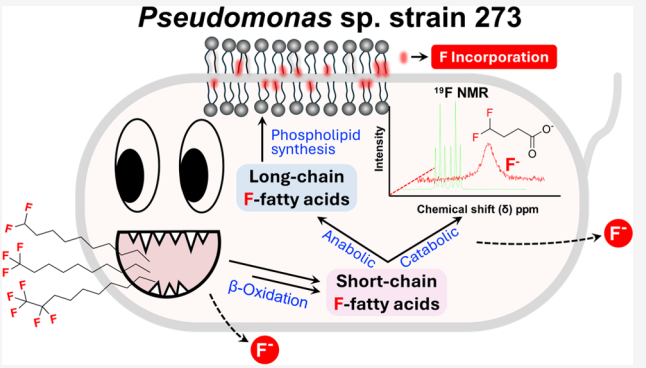

KEYWORDS: *Pseudomonas sp. strain 273, polyfluorinated alkanes, per- and polyfluoroalkyl substances (PFASs), metabolism, defluorination, fluorinated glycerophospholipids, fluoromembrane biosynthesis*

INTRODUCTION

Per- and polyfluoroalkyl substances (PFASs) are recalcitrant, inert, and applied broadly in many sectors. PFASs have become globally distributed, and there is concern that some congeners may impact environmental and human health.[1−5] The strength of the C−F bond was used to explain poor microbial biodegradability of PFASs;[6] however, microbial enzymes have been demonstrated to break C−F bonds at room temperature and neutral pH.[7−12] More likely, the observed recalcitrance is attributed to the occurrence of multiple C−F bonds on the same molecule, and the xenobiotic nature of organic compounds with poly- and perfluorinated carbons.[13,14] Many PFASs possess functional groups as an entry point for transformation reactions that can result in the elimination of fluorine in the form of inorganic fluoride.[6]

The soil bacterium *Pseudomonas* sp. strain 273 metabolizes terminally monofluorinated medium-chain length alkanes with concomitant release of inorganic fluoride.[15] A novel type of alkane monooxygenase (AlkB) system attacks the terminally fluorinated carbon to form an unstable geminal halohydrin that eliminates fluoride to form an aldehyde that is subsequently oxidized to a carboxylate.[16,17] If the initial oxidation occurs on the nonfluorinated terminus, or if the substrate bears fluorines at both termini, monofluorinated fatty acids are produced.[15,18] The catabolism of monofluorinated fatty acids generates fluorinated intermediates that can enter anabolic pathways resulting in the synthesis of fluorinated glycerophospholipids that are incorporated into membrane structures (e.g., the membrane bilayer) of strain 273.[18]

This study investigates the ability of *Pseudomonas* sp. strain 273 to metabolize polyfluorinated decanes and explores fluoromembrane formation in response to increasing levels of fluorination at one terminal end of the decane substrate. Growth studies demonstrate that *Pseudomonas* sp. strain 273 utilizes *n*-decanes with terminal $-CF_2H$, $-CF_3$, and $-CF_2-CF_3$ groups as

Received: May 20, 2025
Revised: September 25, 2025
Accepted: September 26, 2025
Published: October 15, 2025

https://doi.org/10.1021/acs.est.5c06771
Environ. Sci. Technol. 2025, 59, 22663−22675

growth substrates under oxic conditions. The integrated application of ^{19}F NMR, ultrahigh performance liquid chromatography-high resolution mass spectrometry (UHPLC-HRMS), UHPLC-MS/HRMS, gas chromatography-MS (GC-MS), and fluoride ion selective electrode analysis identified transformation products and revealed catabolic pathways for F2-decane, F3-decane, and F5-decane, and demonstrated variation in organofluorine incorporation into different glycerophospholipid classes based on the degree of fluorination of the growth substrate.

MATERIALS AND METHODS

Chemicals. 1,1-Difluorodecane (F2-decane, purity >97%), 1,1,1-trifluorodecane (F3-decane, purity >96%), 1,1,1,2,2-pentafluorodecane (F5-decane, purity >97%), 4,4-difluorobutanoic acid (purity >97%) and 5,5,6,6,6-pentafluorohexanoic acid (purity >97%) were obtained from SynQuest Laboratories, Inc. (Alachua, FL, USA). Decanoic acid (purity >99.5%), trifluoroacetic acid (TFA) (purity >99%), potassium fluoride (purity >99%), *n*-decane (decane) (purity >99%), sodium 4,4,4-trifluorobutanoate (F3-butanoate, purity >97%), 6,6,6-trifluorohexanoic acid (purity >95%) standards, and hexanes (purity >97%) were obtained from Sigma-Aldrich (St. Louis, MO, USA). Glycerophospholipid standards (SPLASH LIPIDOMIX Mass Spec Standard, 330707) were obtained from Avanti Polar Lipids, Inc. (Alabaster, AL, USA). Ethanol (purity >99.5%), diethyl ether (purity >99%), pyridine (purity >99%), *n*-propanol (purity > (99.9%), propyl chloroformate (purity >98%), ammonium hydroxide and methanol (purity >99.8%) were obtained from Fisher Scientific (Waltham, MA, USA). All other chemicals used were analytical reagent grade or higher, unless otherwise specified. All decanes were unbranched *n*-decanes. All substrates were confirmed to be free of fluorinated impurities by ^{19}F NMR before incubation with strain 273, and initial ^{19}F NMR spectra collected from newly established incubations also did not detect any fluoride or fluorinated impurities.

Growth Conditions of *Pseudomonas* sp. Strain 273. Strain 273 was grown in defined phosphate-buffered (pH 7.3) mineral salt medium.[15] To test growth with different polyfluorinated decanes, strain 273 was grown for two consecutive transfers with 7 mM decanoate added gravimetrically, before fresh medium vessels received 0.5% (v/v) of a strain 273 suspension with an optical density ($OD_{600\ nm}$) of l.0 as inoculum. The fresh medium contained 7 mM (nominal) of a fluorinated decane or decane. Liquid alkanes were added gravimetrically using a glass microsyringe. For lipidomic measurements, cultures were grown in 50 mL baffled Erlenmeyer flasks (Sigma, St. Louis, MO, USA) containing 10 mL of medium and sealed with rubber stoppers (Supelco; Stockbridge, GA, USA) held in place with tape. Quintuplet vessels were pressurized with 1.5 atm of air to provide oxygen as electron acceptor. Incubation occurred at 30 °C in the upright position at 120 rpm. Cultures grown with F2-deane, F3-decane, and F5-decane were harvested for lipid extraction following complete consumption of the fluorodecane substrate based on GC-MS measurements (12-h incubation for F3-decane and F5-decane; 20-h incubation for F2-decane). To determine mass balances, strain 273 was grown in quintuplet sealed 160 mL glass serum bottles containing 10 mL of medium that received 7 mM (nominal) of a polyfluorodecane under an air headspace of 2 atm. The cultures were incubated for 4 days (F2-decane/F3-decane/F5-decane) and 14 days (F5-decane +10 mM decanoate) prior to quantitative analysis of substrates and products.

ANALYTICAL PROCEDURES

Quantification of Growth Substrates and Fluorinated Short-Chain Fatty Acids. Analysis of short chain fatty acids and growth substrates was performed using an Agilent 5977 GC coupled to a mass-selective detector equipped with an Agilent HP-5MS Ultra Inert 30 m x 250 μm x 0.25 μm column (Santa Clara, CA) (Supporting Methods; SI). Quantification of initial substrate concentrations was performed via hexanes extraction of 1 mL culture suspension samples collected immediately after inoculation and vigorous agitation. External standard curves were prepared by mixing different volumes of F2-decane, F3-decane, or F5-decane with hexanes to obtain a concentration of ~7 mM, with a range of starting concentrations between 7.02 ± 0.08 to 7.79 ± 0.08 mM. These stock solutions underwent a series of half log dilutions (~7 mM − 0.07 mM) in hexanes to generate standard curves covering the desired concentration ranges.[19] No measurements in this study had a peak with a signal-to-noise ratio <3:1. Therefore, the limit of detection (LOD) and the limit of quantification (LOQ) were assumed to be the lowest concentrations from the calibration data, which averaged ~0.073 mM. Quantification of fluorinated short-chain fatty acids followed an established derivatization procedure.[20] Briefly, cultivation vessels were placed in −80 °C for 5 min to condense all volatile compounds. One mL culture suspension samples were withdrawn from the cultivation vessels (five replicates per growth substrate), mixed with 250 μL *n*-propanol/pyridine (3:2, v:v) solution in 2 mL plastic Eppendorf tubes, followed by the addition of 50 μL propyl chloroformate. The tubes were vortexed briefly and vented, followed by a 30-s treatment in an ultrasonic water bath. Hexanes (300 μL) was added to each tube, immediately vortexed, and centrifuged at 3,000 x *g* for 3 min at room temperature. The top layers (~300 μL) were transferred to 300 μL glass autosampler vials, which were closed and stored at 4 °C until analysis. Abiotic control incubations without inocula (three replicates per substrate), each containing 7 mM of potential fluorinated short-chain fatty acid transformation products (i.e., F2-butanoate, F3-butanoate, and F5-hexanoate), were incubated alongside live cultures to assess abiotic losses and generate external standard curves (7 mM − 0.086 mM) for short-chain fatty acid quantification[21,22] (Figures S1 and S2). Additional information regarding the quantification of short-chain fatty acids and initial substrates can be found in SI Figures S1 and S2 and Tables S1−S4.

^{19}F NMR Spectroscopy. NMR spectra were acquired with a Varian VNMRS 470 MHz (Palo Alto, CA, USA) and a Bruker Avance NEO 470 MHz (Billerica, MA, USA) nuclear magnetic resonance spectrometers. The Varian was equipped with a OneNMR probe (Agilent, Santa Clara, CA) channeled to fluorine, and the Bruker was fitted with a Broad Band probe to observe fluorine. A limit of detection of 5 μM (~0.1 mg L^{-1}) inorganic fluoride was established using a maximum of 1,000 scans. The spectra produced in this investigation were fluorine-proton coupled and fluorine−fluorine coupled. The 5 mm diameter NMR tube (CortecNet, Brooklyn, NY, USA) containing a 1 mM sodium trifluoroacetate (TFA) internal standard dissolved in deuterium oxide (Cambridge Isotope Laboratories, Tewksbury, MA, USA) was placed within a glass capillary and sealed at both ends. For ^{19}F NMR analysis, 10 mL cultures were grown in 50 mL baffled Erlenmeyer flasks with the respective polyfluorinated decane (7 mM, nominal). For ^{19}F

https://doi.org/10.1021/acs.est.5c06771
Environ. Sci. Technol. 2025, 59, 22663−22675

NMR analysis, 800 μL of culture suspension was transferred to the NMR tube followed by the insertion of a 1 mM TFA internal standard sealed within a separate glass capillary. Scans were collected from samples taken immediately after inoculation, after 4 days (F2-decane, F3-decane, and F5-decane), and after 14 days (F5-decane + decanoate) of incubation. Whole cell ^{19}F NMR was performed to determine consumption of fluoroalkane substrates, assess defluorination (i.e., formation of inorganic fluoride), and to identify fluorinated metabolites. Full ^{19}F NMR spectra were collected from δ + 20 to −200 ppm and can be found in the SI (Figures SA1−SA28). Spectra of unknown compounds were matched to authentic standards (unless unavailable) with further identity confirmation using GC-MS (Figure S3). Abiotic control incubations without inocula (triplicates per substrate), each containing 7 mM of substrate (F2-decane, F3-butanoate, F5-hexanoate, or F5-decane), were incubated alongside live cultures to assess abiotic losses (Figure S4).

Fluoride Measurements. Inorganic fluoride concentrations were calculated using data obtained from ^{19}F NMR [eqs 1−3 (SI)]. In addition, fluoride was quantified with an Orion Star A214 benchtop meter equipped with a fluoride ion-selective electrode (FISE) (IonPlus SureFlow 9609BNWP). An external standard curve was generated with a series of potassium fluoride solutions (half log dilutions; 7 mM − 0.01 mM) following the electrode manufacturer's guidelines. Concentrations were determined using eqs 4 and 5 (SI) and are shown in Figures S5 and S6 and Table S6.

Quantitative PCR (qPCR). For enumeration of strain 273 cells, 1 mL culture suspension aliquots were passed through 0.22 μM polyvinylidene difluoride membrane filters (Merck Millipore Ltd., Burlington, MA, USA). Genomic DNA was extracted from the cells captured on the filters using the DNeasy PowerLyzer PowerSoil kit (Qiagen, Hilden, Germany). SYBR Green-based qPCR followed an established protocol using primers (5′-3′) F-GCTAGTCTAACCTTCGGGGG (Tm = 59 °C) and R-TCCCCTACGGCTACCTTGTT (Tm = 60 °C) targeting a consensus region of the five 16S rRNA genes of strain 273.[18,23] Strain 273 possesses five 16S rRNA genes per genome, and cell abundances were calculated by dividing the 16S rRNA gene copy numbers by a factor of 5.[24]

Chromatographic Methods for Glycerophospholipid Measurements. For the analysis of cellular glycerophospholipids, a two-pronged approach was applied involving hydrophilic interaction liquid chromatography (HILIC) (Method H),[25,26] and reversed-phase (RP) chromatography (Method RP).[27] Method H achieves global lipidome profiling and identifies fluorinated glycerophospholipids through separation via headgroup to match retention times. Method RP also achieves global lipidome profiling, but also generates information about sn1/sn2 glycerophospholipid acyl chain fragmentation signatures.[28] See SI for detailed protocol for glycerophospholipid extraction.

Data Analysis. Nonfluorinated glycerophospholipids were annotated using a library of formulae that allowed for 6−46 carbons in the fatty acyl tails and up to 10 degrees of unsaturation among the two tails. At least one standard for each major phospholipid class was used in the analyses, and structures were further validated with fragmentation when available. Fluorinated glycerophospholipids were annotated using a custom library comprising all possible formulae above with 1 to 10 fluorine substitutions added, retention time matches to the respective nonfluorinated internal standards (± 0.5 min), and mass accuracies (± 5 ppm) of the expected m/z values. The structure of annotated fluorinated glycerophospholipids were further validated using fragmentation data when available. Since standards of fluorinated glycerophospholipids are not available, retention times of these analytes were estimated based on those observed for the respective nonfluorinated analogs operated using Method H on an Orbitrap Exploris 120. A total glycerophospholipid detected (%) figure was constructed by summing individual concentrations of detected glycerophospholipids by specific categories and presenting respective glycerophospholipid classes as a percentage of total ions detected. Glycerophospholipid abundances were determined by summation of the relative concentrations by comparison to the Avanti deuterated internal standard. A heatmap was developed that summed fluorinated species and nonfluorinated species and calculated the ratio of normalized, $\log_2$ transformed intensities of F2-decane, F3-decane, and F5-decane-grown cells over decane grown-cells and clustered using RStudio (V2024.12.1) (Posit Software, PBC, Boston, MA, http://www.posit.co/). A paired student's t-test was utilized to determine significance and calculate p-values. Relative concentration estimates of fluorinated glycerophospholipids assumed that fluorinated glycerophospholipids and their nonfluorinated counterparts had the same ionization efficiency, resulting in comparable peak areas and signal intensities. Abundance data represent the averages of five biological replicates. The mass spectra and extracted io chromatograms were plotted using XCalibur software version 4.2 SP1 (Thermo Fisher Scientific). Additional information regarding UHPLC-HRMS methods and specific parameters can be found in the Supporting Methods in the SI.

RESULTS

***Pseudomonas* sp. Strain 273 Catabolizes *n*-Decanes Carrying Poly- or Perfluorinated Carbon Atoms.** *Pseudomonas* sp. strain 273 grew with F2-decane, F3-decane, or F5-decane under oxic conditions as determined by substrate consumption, formation of fluorinated catabolites, and increase in cell density (determined with qPCR, Table S5). After a 4-day incubation, strain 273 consumed 7.15 ± 0.17 mM F2-decane or 7.53 ± 0.72 mM F3-decane to below detectable levels, generating 6.39 ± 0.19 mM F2-butanoate or 6.13 ± 0.28 mM F3-butanoate, respectively, as a major catabolite (Figure 1A, B). During growth with F2-decane, 0.17 ± 0.04 mM inorganic fluoride was released (Figure 1A) indicating some C−F bond cleavage; however, fluoride release was not apparent with F3-decane as a growth substrate (Figure 1B, Table S6). Cultures that received 7.00 ± 0.21 mM F5-decane produced 0.48 ± 0.28 mM F5-hexanoate as the only catabolite detected without measurable fluoride release (Figure 1C). Interestingly, fluoride release was observed in strain 273 cultures amended with F5-decane and decanoate as additional growth substrate. Following an extended 14-day incubation, cultures with 7.08 ± 0.14 mM F5-decane and 10 mM decanoate generated 1.44 ± 0.47 mM F3-butanoate and 0.226 ± 0.132 mM F5-hexanoate associated with the release of 2.72 ± 0.91 mM fluoride (Figure 1D). No growth or fluoride release occurred in abiotic controls with carbon substrate and no inoculum or vessels with inoculum and no carbon substrate (Figure S4, Tables S6 and S7).

Confirmation and Identification of Polyfluorinated Catabolites and Inorganic Fluoride via ^{19}F NMR. To obtain more information about the catabolites formed, ^{19}F NMR analysis was performed on live strain 273 culture suspensions.

https://doi.org/10.1021/acs.est.5c06771
Environ. Sci. Technol. 2025, 59, 22663−22675

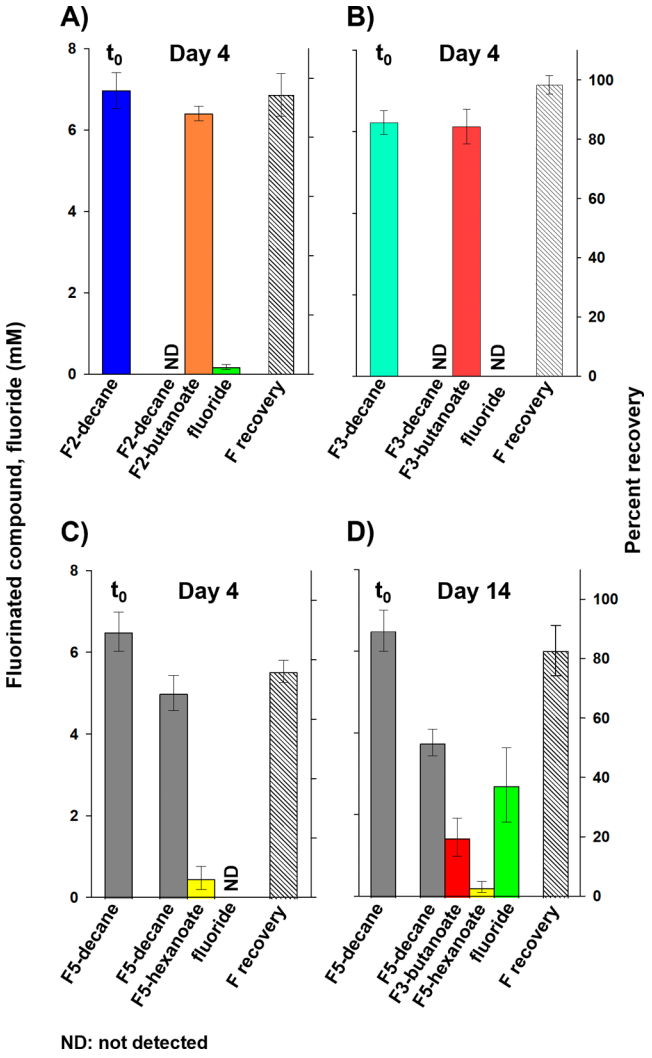

Figure 1. Mass balance analysis of fluorodecane substrates and product(s) in cultures of *Pseudomonas* sp. strain 273 immediately following inoculation (t_0) and after specified incubation periods. Each panel plots the initial substrate concentration (far left), the corresponding fluorinated products (middle), and % fluorine recovered (far right). Colors are conserved across all panels: fluoride (green), F3-butanoate (red), F5-hexanoate (yellow), F5-decane (gray), and total fluorine recovery (hatched fill pattern). Error bars represent the standard deviations observed for quintuplet cultures per treatment. ND = not detected. Growth with F2-decane resulted in the formation of F2-butanoate and a small amount of inorganic fluoride after 4 days with a percent recovery of 96.0 ± 2.9% (Panel A). Growth with F3-decane resulted in the formation of F3-butanoate and no fluoride release after 4 days with a percent recovery of 98.4 ± 3.1% (Panel B). Growth with F5-decane resulted in F5-hexanoate formation but no fluoride release after 4 days with a percent recovery of 76.2 ± 3.7% (Panel C). The addition of decanoate stimulated F5-decane degradation and resulted in the production of inorganic fluoride and F3-butanoate in a ratio of ~2:1 (Panel D) with a percent recovery of 82.7 ± 8.5%. Initial (t_0) recoveries of substrates, recoveries of polyfluorinated catabolites and fluoride after specified incubation periods (t_1, 4 or 14 days), and cell densities are shown in Figures S1, S2, and S6 and Tables S1−S7. As the detected molecules contained differing numbers of F, the mol of F contained in each organic or inorganic species was determined by multiplying the concentration of each substrate and transformation product by the number of fluorines in the respective molecules to facilitate accurate flouride and organic fluoride recovery (F Recovery) calculations. Therefore, total F Recovery for each experimental condition was calculated using the following formula: F Recovery Percentage = $(\Sigma_{i=0}^{n}[\text{organofluorine product(s)}]_{i=1} \times \#F + [F^-])/([\text{organofluorine substrate}]_{i=0} \times \#F) \times 100$.

The ^{19}F NMR data shown in Figure 2A display the initial conditions with 7 mM (nominal) F2-decane (δ −117.4 ppm). Following a 4-day incubation, ^{19}F NMR revealed a shift of δ 0.2 ppm from F2-decane indicative of the formation of F2-butanoate (δ −117.6 ppm, Figure 2B) (Figures S3 and S4). ^{19}F NMR confirmed the FISE measurements and detected the release of inorganic fluoride in F2-decane-grown cultures (Table S7). A 4-day incubation of F3-decane-grown strain 273 cells revealed a shift of δ 1.3 ppm from the F3-decane substrate (δ −68.8 ppm, triplet), indicating F3-butanoate (δ −67.5 ppm) formation (Figure 2C,D). ^{19}F NMR did not detect fluoride in F3-decane-grown cells demonstrating no C−F bond cleavage occurred (Figure 2D, Figures S3 and S4). Cells grown with F5-decane and decanoate produced F5-hexanoate and F3-butanoate, as confirmed with ^{19}F NMR (Figures S3 and S4). The use of ^{19}F NMR detected inorganic fluoride (δ −120.2 ppm, singlet) (Figure 2F, Figures S3 and S4 and Table S7). ^{19}F NMR performed on strain 273 cultures grown with F5-decane and decanoate identified several organofluorine catabolites in low abundances (Figure 2F). Notably, a peak detected as a triplet (δ −66.9 ppm) was similar in chemical shift to 6,6,6-trifluorohexanoate (F3-hexanoate: δ −66.8 ppm) based on comparison to an authentic external standard (Figure S3) and separated by δ 0.10 ppm. The molecule has been annotated as 6,6,6-trifluoro-3-oxohexanoate since the shift matches that expected from a carbonyl three carbons away from the terminal carboxylate. Quantification of F2-butanoate and F3-butanoate with ^{19}F NMR was lower than expected presumably due to loss of volatile polyfluorinated butyric acids during transfer of live culture suspensions into the NMR tubes. Alkyl carboxylic acid have been shown to form azeotropes with water and alcohols,[29] and fluorination is known to lower the boiling points of molecules.[30] The NMR analysis of cultures amended with F5-decane did not detect this molecule following a 4-day (Figure 2F) and 14-day (Figure 2H) incubation due to consumption, presumed volatility, (Figures S7 and S8), and/or poor solubility (i.e., a separate, immiscible nonaqueous phase liquid [NAPL] phase was observed following the 4- and 14-day incubation periods) of this compound.

Product(s) of F5-Decane Catabolism. When strain 273 culturs were amended with F5-decane as the sole substrate, F5-hexanoate was the only detectable catabolite during a 4-day incubation (Figure 1C). When F5-decane was coamended with decanoate, F5-hexanoate plus two additional fluorinated products, F3-butanoate and fluoride were detected (Figure 1D). Assuming F5-hexanoate is the precursor to F3-butanoate, the loss of the methylene fluorines ($-CF_2-$) of F5-hexanoate (δ-carbon) can occur via two HF eliminations resulting in the β-oxidation intermediate 6,6,6-trifluoro-3-oxohexanoate. Such a reaction would lead to a 2:1 mixture of fluoride:F3-hexanoate (Figure 1D). To determine if F5-hexanoate was the substrate for defluorination and a precursor of F3-butanoate, strain 273 cultures were grown with 10 mM decanoate in the presence of 7.16 ± 0.160 mM F5-hexanoate. Fluoride release and F3-butanoate production were observed in these cultures (Figure 3B, Table S7) consistent with the postulated reaction sequence. Notably, ^{19}F NMR analysis of cultures that received F5-

https://doi.org/10.1021/acs.est.5c06771
Environ. Sci. Technol. 2025, 59, 22663−22675

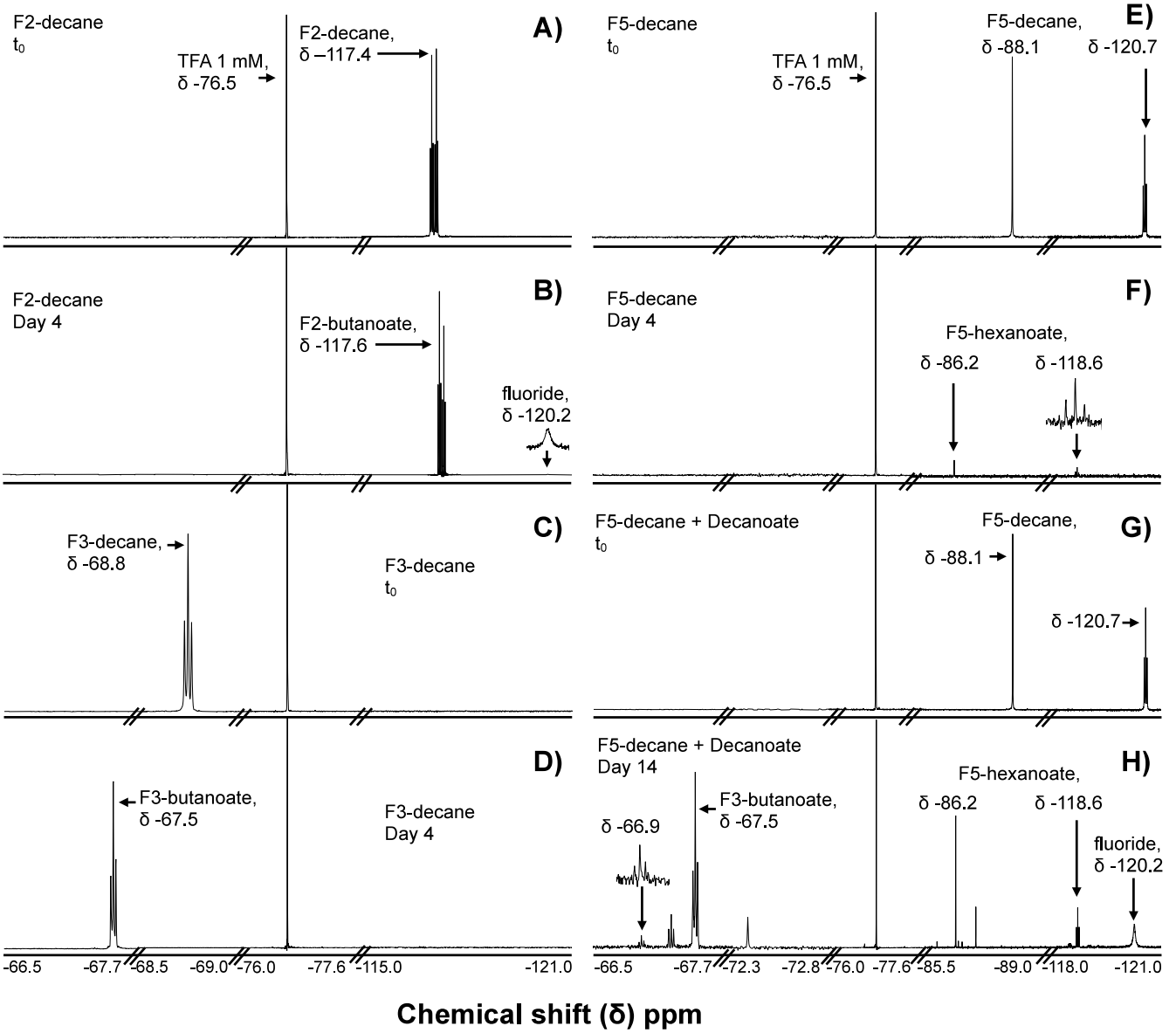

Figure 2. ^{19}F NMR analysis of strain 273 live culture suspensions amended with F2-decane, F3-decane, F5-decane, or F5-decane + decanoate immediately following inoculation (t_0) and after specified incubation periods. Panel A illustrates the spectrum for F2-decane (δ −117.4 ppm) at t_0. Panel B shows the formation of F2-butanoate (δ −117.6 ppm) after a 4-day incubation. Panel C shows t_0 for cells grown with F3-decane (δ −68.8 ppm), and Panel D depicts the formation of F3-butanoate (δ −67.5 ppm) after 4 days. Panel E shows the t_0 spectrum for F5-decane-grown cells (δ −88.1 singlet, −120.7 triplet ppm). Panel F depicts F5-hexanoate formation (δ −86.2 singlet, −118.6 triplet ppm) following a 4-day incubation period with F5-decane. Panel G shows the t_0 spectrum for cultures that received F5-decane + decanoate-grown cultures (δ −88.1 singlet, −120.7 triplet ppm). Panel H depicts both identified and unidentified fluorinated catabolites following a 14-day incubation period with F5-decane + decanoate. All named compounds were identified based on comparisons to authentic external standards (Figure S3). Quantification via the 1 mM TFA internal standard revealed no more than 2.78 ± 0.910 mM inorganic fluoride release that coincided with 1.44 ± 0.470 mM F3-butanoate formation in F5-decane + decanoate-grown cultures (Table S7). Quantification of solutes was performed using eqs 1−5 (SI). Control incubations containing F2-decane, F3-decane, or F5-decane demonstrated no fluoride release or degradation after the growth period (Figure S4). Each spectrum ranges from δ −66.5 to −121.0 ppm with axis breaks (//) removing regions where no peaks were detected.

hexanoate + decanoate detected a peak (δ −66.9 ppm, triplet), which was also observed in cell suspensions grown with F5-decane + decanoate. To determine if F3-hexanoate was a substrate for β-oxidation and a precursor of F3-butanoate, strain 273 cultures were grown with 1 mM F3-hexanoate (Figure 3C). The ^{19}F NMR analysis of cultures that received F3-hexanoate as the sole carbon substrate identified F3-butanoate (δ −67.5 ppm, triplet) as catabolic product following a 60-day incubation. These experiments suggest that F5-decane is converted to F5-hexanoate via two subsequent β-oxidation cycles. F5-hexanoate then undergoes defluorination at the perfluorinated δ-carbon ($-CF_2-$) to generate a structure similar to F3-hexanoate, which ^{19}F NMR analysis tentatively identified as 6,6,6-trifluoro-3-oxohexanoate based on the chemical shift. One additional cycle of β-oxidation would yield F3-butanoate. Taken together, these findings illustrate the capability of strain 273 to defluorinate the perfluorinated δ-carbon ($-CF_2-$) of F5-hexanoate, resulting in the formation of F3-butanoate and inorganic fluoride.

Detection and Identification of Fluorinated Glycerophospholipids. Utilizing Method H, polyfluorinated glycer-

https://doi.org/10.1021/acs.est.5c06771
Environ. Sci. Technol. 2025, 59, 22663−22675

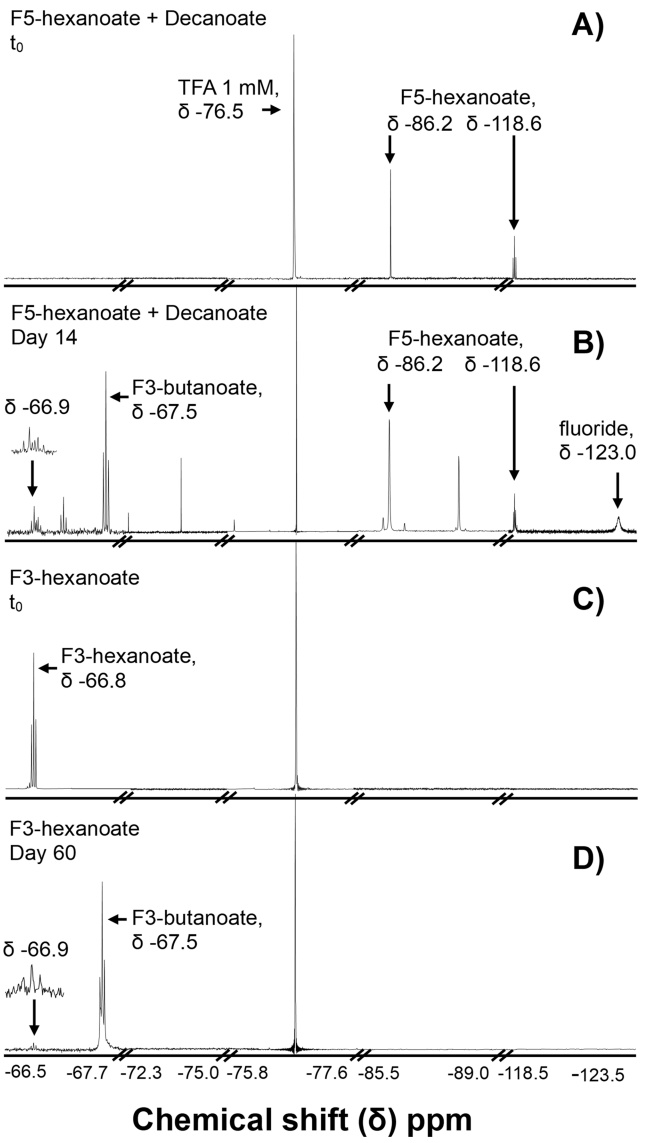

Figure 3. ^{19}F NMR analysis of medium amended with F5-hexanoate + decanoate immediately following inoculation (t_0) with strain 273 and after a 14-day incubation period. Panel A illustrates the t_0 ^{19}F NMR spectrum for the F5-hexanoate + decanoate growth condition (δ −86.2 singlet, −118.6 triplet ppm). Panel B shows the formation of F3-butanoate (δ −67.5 ppm, triplet) with corresponding fluoride release (δ −123.0 ppm, singlet) and a F3-hexanoate peak (δ −66.9 ppm, triplet) following a 14-day incubation period. Panel C illustrates the t_0 ^{19}F NMR spectrum for strain 273 culture suspensions amended with F3-hexanoate (δ −66.8 ppm, triplet) as the sole growth substrate. Panel D shows the formation of F3-butanoate (δ −67.5 ppm, triplet) with only a minor amount of F3-hexanoate remaining following a 60-day incubation period. All compounds were identified based on comparison to authentic external standards dissolved in the defined medium (Figure S3). Each spectrum ranges from δ −66.5 to −123.5 ppm with axis breaks (//) to remove regions where no peaks were detected.

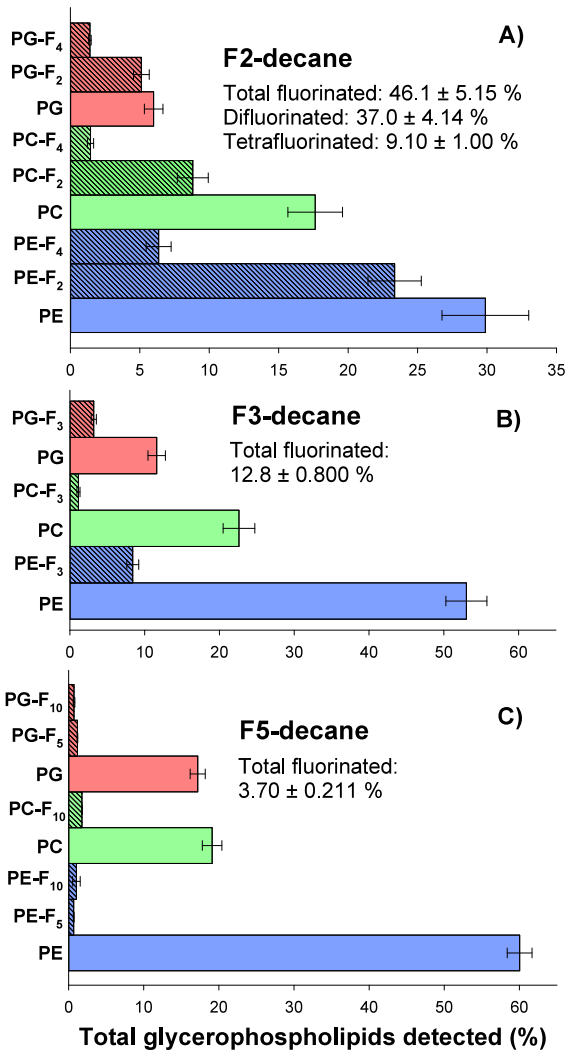

Figure 4. Percentages of fluorinated (shaded bars) and nonfluorinated (solid bars) glycerophospholipids measured in *Pseudomonas* sp. strain 273 cells grown with F2-decane, F3-decane, or F5-decane as the sole carbon substrates. Organofluorination of glycerophospholipids is shown as a percentage of all detected lipids arranged by major glycerophospholipid classes (i.e., PE, PG, and PC) and their fluorinated counterparts. Each bar plot represents 100% of all detected glycerophospholipids for each growth substrate (i.e., F2-decane, F3-decane, or F5-decane) and includes data from five replicate cultures. Error bars represent the standard deviations. See SI for calculation of percent distribution per glycerophospholipid class (eqs 6−11 in SI) and relative glycerophospholipid abundance information (Figure S9, Tables S8−S12).

ophospholipids were identified and quantified in strain 273 cells grown with polyfluorinated decanes. Fluorinated phosphatidylcholines (PCs) were in highest relative abundance in F2-decane-grown cells (Figure 4A). The relative abundance of fluorinated lipids decreased in the order F2-decane > F3-decane > F5-decane) indicating a shift in fluorinated glycerophospholipid incorporation into the membrane bilayer with respect to the degree of fluorination of the growth substrate (Figure 4). With F2-decane as growth substrate, 37.0% of all detected glycerophospholipids possess two fluorine substitutions on a single acyl chain (difluorinated glycerophospholipid species) with an additional 9.10% possessing two fluorine substitutions on each of the sn1 and sn2 acyl chains (tetrafluorinated glycerophospholipid species) (Figure 4A). Total organofluorine incorporation decreased to 12.8% in cells grown with F3-decane with single fluoroacyl chains detected and hexafluorination (i.e., three fluorine substitutions on each of the sn1 and sn2 acyl chains) was not observed. Of all fluorinated decane growth substrates, organofluorine incorporation into the lipidome was lowest in cells grown with F5-decane (3.70%) with glycer-

https://doi.org/10.1021/acs.est.5c06771
Environ. Sci. Technol. 2025, 59, 22663−22675

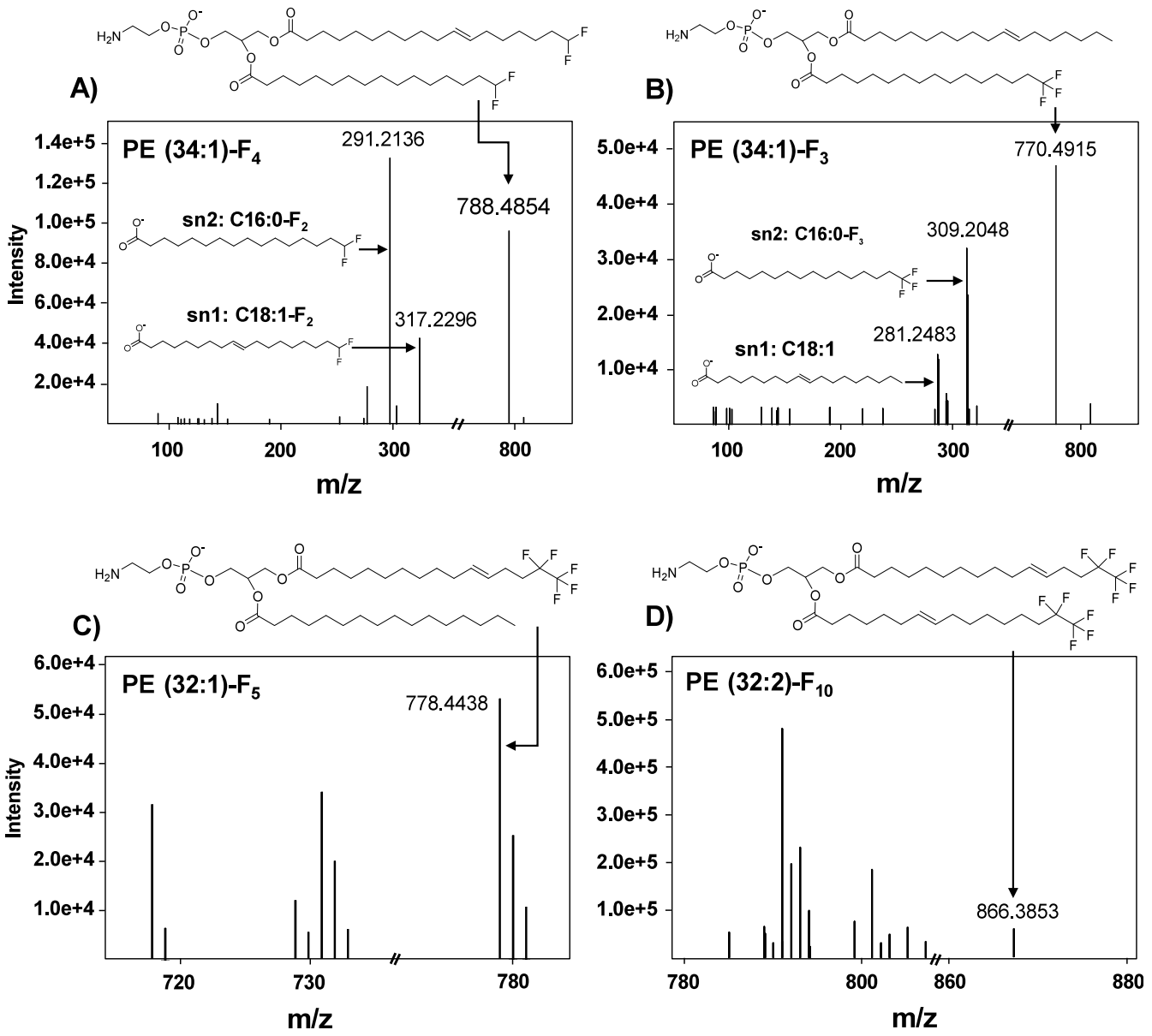

Figure 5. UHPLC-MS/HRMS analysis of glycerophospholipid extracts from strain 273 cells grown with F2-decane, F3-decane, or F5-decane. Panel A shows the mass spectrum and identification of a tetrafluorinated PE (34:1)-F_4 (negative mode) from F2-decane-grown cells, demonstrating difluorination of both the sn1 (C18:1-F_2) and the sn2 (C16:0-F_2) acyl chains. Panel B shows the mass spectrum and identification of a trifluorinated PE (34:1)-F_3 (negative mode) from F3-decane-grown cells, demonstrating a trifluorinated methyl group on the sn2 acyl chain. Panel C shows the mass spectrum and identification of PE (32:1)-F_5 in lipid extracts from F5-decane-grown cells, demonstrating incorporation of a pentafluorine moiety on a single acyl chain. Panel D shows the mass spectrum and identification of PE (32:2)-F_{10} (negative mode) from F5-decane-grown cells, demonstrating incorporation of a pentafluorine moiety on both acyl chains can occur. Positions of unsaturations and organofluorine group distribution between sn1 and sn2 acyl chains are unknown, and the lipid structures are representations of possible configurations. Specific fatty acyl chain lengths in panels C and D are inferred from the preference of strain 273 to produce the nonfluorinated analogues of these fatty acids. Unlabeled peaks could represent unidentified glycerophospholipids or fragments of glycerophospholipids, such as the headgroup.

ophospholipids possibly possessing a single or two pentafluorinated acyl chains observed based on retention time and *m*/*z*.

Comparative analyses revealed an uneven distribution of organofluorine incorporation throughout the lipidome (i.e., fluorination of different glycerophospholipid classes), relative to the degree of fluorine substitution on the fluorinated decane growth substrate (Figure 4). Organofluorine incorporation preference is exemplified for strain 273 cells grown with F2-decane, demonstrating a higher abundance of di- and tetrafluorinated phosphatidylethanolamine (PE) and phosphatidylglycerol (PG) compared to PC (Figure 4A). More specifically, the combination of PG-F_4 and PG-F_2 (6.50%) accounted for a slightly higher percent abundance than nonfluorinated PG (6.00%) for F2-decane grown cells (Figure 1A). Similarly, the relative abundance of fluorinated PEs (∼30.0%) to nonfluorinated PEs (∼30.0%) was equal (Figure 1A). However, organofluorine glycerophospholipid preference is observed for PC, with more nonfluorinated PCs (∼18.0%) than fluorinated PCs (PC-F_2 + PC-F_4; 10%) being detected. For F3-decane-grown cells, PGs were the most frequently detected fluorinated glycerophospholipid, despite being the least abundant glycerophospholipid class (Figure 4B). Organo-

https://doi.org/10.1021/acs.est.5c06771
Environ. Sci. Technol. 2025, 59, 22663−22675

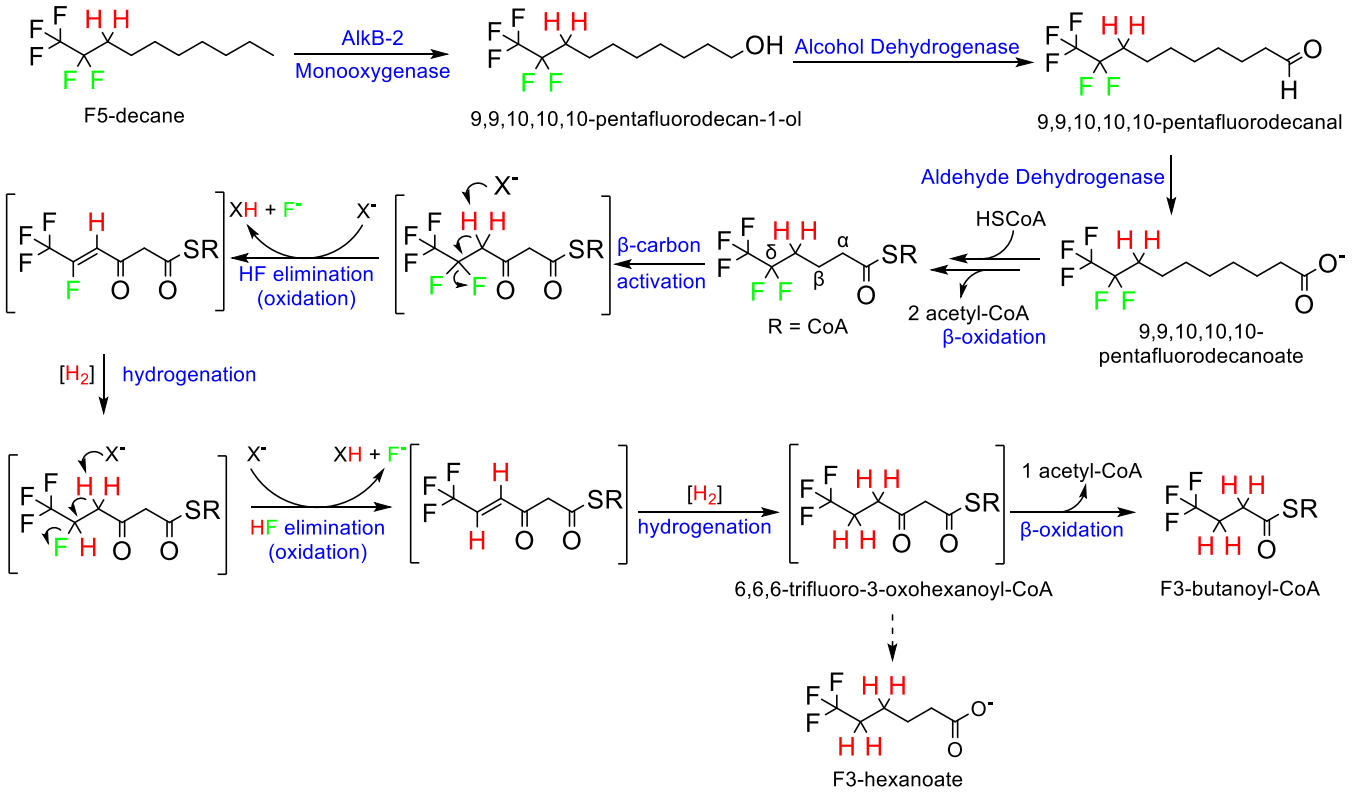

Figure 6. Proposed pathway for the catabolic conversion of F5-decane to F3-butanoate in *Pseudomonas* sp. strain 273. AlkB-2 oxidizes F5-decane to 9,9,10,10,10-pentafluorodecan-1-ol, which is further oxidized via the aldehyde to the carboxylate. Two cycles of β-oxidation result in the formation of F5-hexanoate, which undergoes activation at the β carbon followed by HF elimination. Two subsequent oxidation/hydrogenation reactions liberate inorganic fluoride from the perfluorinated δ-carbon ($-CF_2-$) and yield 6,6,6-trifluoro-3-oxohexanoate, which undergoes one additional cycle of β-oxidation to form F3-butanoate. The proposed pathway generates inorganic fluoride and F3-butanoate in a 2:1 ratio, consistent with the experimental observations during growth of strain 273 with F5-decane + decanoate. The letters X and Y represent unknown hydrogen/electron carriers. Under in vivo conditions, the deprotonated carboxylates exist as CoA thioesters ("R").

fluorine incorporation preference during growth with F5-decane was not apparent, presumably due to the low overall abundance of acyl chains with pentafluorination (Figure 4C).

Utilizing Method RP, multiple fluorinated glycerophospholipids were classified by retention time, exact mass (±5 ppm) to constrain the formulas and predict combined fatty acyl tail length, and fragmentation data, if available, to identify specific fatty acyl tail moieties. The UHPLC-HRMS measurements identified compounds with m/z ratios consistent with difluorinated sn1/sn2 acyl chains in cells grown with F2-decane (Figure 5A). The UHPLC-MS/HRMS fragmentation data for samples from F2-decane-grown strain 273 cells indicate that glycerophospholipids can possess a maximum of four organofluorine substitutions by incorporating two organofluorines on both the sn1 and sn2 acyl chains (Figure 5A). Similarly, the UHPLC-MS/HRMS data for samples from F3-decane-grown cells possess m/z ratios consistent with a single trifluoromethyl group located on the sn1 or the sn2 acyl chain (Figure 5B). These results suggest strain 273 can incorporate a single trifluoromethyl group into a glycerophospholipid when grown with F3-decane. Hexafluorinated glycerophospholipids (i.e., each acyl chain carrying a trifluoromethyl group) were not observed in cells grown with F3-decane. UHPLC-MS/HRMS analysis of samples from cells grown with F5-decane identified glycerophospholipid classes with both five and ten fluorine substitutions, albeit in low abundances (Figure 5C,D). Fragmentation of sn1/sn2 acyl chains (Method RP) could not be achieved for highly fluorinated lipids due to their low relative abundances in cells grown with F5-decane, and the identification of these molecules was based on expected retention time and exact mass (±5 ppm, Figure 5C,D).

DISCUSSION

Despite the recalcitrance reported for many fluorinated xenobiotics, microbial degradation and defluorination of fluorinated compounds has been observed.[12,31−37] Recent work demonstrated that some *Pseudomonas* spp. possess a unique alkane monooxygenase (AlkB) enzyme system comprising the catalytic AlkB component and a fused ferredoxin - ferredoxin reductase that is involved in the initial attack on terminally monofluorinated alkanes.[16] Interestingly, some defluorinating AlkB enzyme systems have a preference for terminal $-CH_2F$ over the $-CH_3$ group, suggesting they are alkyl fluoride dehalogenases.[15,17,18] When *Pseudomonas* sp. strain 273 was challenged with F2-decane or F3-decane, growth occurred but fluoride release was minimal, suggesting that terminal difluorination ($-CF_2H$) or perfluorination ($-CF_3$) directs the initial AlkB attack to the nonfluorinated end of the fluoroalkane growth substrate. Growth with F2-decane demonstrated that one additional fluorine substitution at the C_1 carbon ($-CF_2H$) compared to $-CH_2F$ directs the AlkB attack to the nonfluorinated terminal $-CH_3$ group, with <1% of the total fluorine released as inorganic fluoride. Terminal perfluorination (i.e., $-CF_3$ group) fully directs the AlkB attack to the nonfluorinated methyl group terminal position (ω-carbon), as demonstrated for F3-decane and F5-decane as growth substrates.

https://doi.org/10.1021/acs.est.5c06771
Environ. Sci. Technol. 2025, 59, 22663−22675

Strain 273 possesses three *alkB* gene clusters, and it is possible that different or multiple *alkB* genes are active during growth with F2-decane, F3-decane, and F5-decane; however, a genome-wide expression analysis has demonstrated that during growth with decane and terminally monofluorinated decanes, a single AlkB (i.e., AlkB-2) which couples with a fused ferredoxin - ferredoxin reductase is expressed.[16] Therefore, it is likely that AlkB-2 is responsible for the initial attack on F2-decane, F3-decane, and F5-decane. Albeit with low efficiency, AlkB-2 can directly attack the $-CF_2H$ group of F2-decane leading to the formation of a halohydrin followed by spontaneous release of one fluorine substituent. In contrast, no fluoride release is observed with F3-decane because direct oxidation of the terminal $-CF_3$ group by AlkB-2 is not possible, and β-oxidation does not produce a transformation product with a carbonyl moiety positioned three atoms away from the $-CF_3$ group, which could allow enolization and subsequent fluoride elimination to occur. Although AlkB-2 cannot attack a $-CF_3$ group, defluorination was observed during growth with F5-decane and likely occurred during the catabolism of shorter-chain fatty acids discussed below. AlkB-2 oxidizes F5-decane to 10,10,10,9,9-pentafluorodecanol, and the alcohol is further oxidized to the carboxylate, activated to its CoA thioester, and then undergoes two cycles of β-oxidation to yield F5-hexanoate. A third cycle of β-oxidation would lead to the formation of 3,3,4,4,4-pentafluorobutanoate; however, the formation of this compound was not observed with F5-decane as the sole growth substrate, possibly because this compound is short-lived and evades detection. Alternatively, a pentafluorinated product of β-oxidation (F5-hexanoate) necessary to produce 3,3,4,4,4-pentafluorobutanoate undergoes defluorination before conversion to a four-carbon fatty acid. Further transformation of F5-hexanoate and a compound similar in chemical shift to F3-hexanoate (tentatively annotated as 6,6,6-trifluoro-3-oxohexanoate) was observed in cultures that received decanoate as an additional growth substrate. Presumably the perfluorinated δ-carbon of F5-hexanoate is defluorinated to this trifluorinated metabolite, indicating a heretofore unrecognized defluorination capability of strain 273. Following the defluorination of F5-hexanoate to 6,6,6-trifluoro-3-oxohexanoate one additional cycle of β-oxidation can occur resulting in the formation of F3-butanoate. Of the 2.70 ± 0.255 mM F5-decane consumed when grown with decanoate, 1.44 ± 0.470 mM (54.4 ± 17.4%) was recovered as F3-butanoate. The enzyme(s) and/or abiotic reaction(s) that convert F5-hexanoate to F3-hexanoate (i.e., defluorination at the δ-carbon) act(s) on a perfluorinated carbon ($-CF_2-$) adjacent to a perfluorinated terminal carbon ($-CF_3$) remain uncharacterized and should be a focus of future investigations. Experimental measurements of carboxylic acids generated from the proposed pathway intermediates and products suggest a biotransformation pathway for F5-decane that produces shorter chain organic acids with fewer fluorines (Figure 6). Notably, the proposed steps of this particular transformation can potentially be accomplished via enzymes needed for fatty acid metabolism of nonfluorinated metabolites.

A similar pathway has been proposed in a study that investigated reactivity relationships in the aerobic defluorination of terminally trifluorinated C_3 and C_5 short chain fatty acids by activated sludge communities.[38] Proposed pathways for the transformation of PFASs often include defluorination of the internal $-CF_2-$ carbon adjacent to the nonfluorinated $-CH_2-$ carbon. Such biotransformation of the $-CF_2-$ group has been observed in sludge and soil microcosms, as well as pure culture incubations with fluorotelomer alcohols [FTOHs, F-$(CF_2)_nCH_2CH_2OH$, n = 4, 6, 8], where the defluorination of multiple $-CF_2-$ groups can result in the formation of shorter chain perfluorinated carboxylic acids (PFCAs).[39−42] Apparently, enzymes catalyzing the defluorination of internal perfluorinated $-CF_2-$ carbons are more broadly distributed, and not a unique feature of *Pseudomonas* sp. strain 273. A prior study observed the microbial biotransformation of aqueous film-forming foam- (AFFF-) derived polyfluoroalkyl substances to 8:2 fluorotelomer carboxylic acid (FTCA), followed by a dehydrohalogenation step involving the loss of the first fluorine at the β-carbon ($-CF_2-$) and one hydrogen from the adjacent carbon ($-CH_2-$), resulting in the formation of 8:2 fluorotelomer unsaturated carboxylic acid (FTUCA).[41] The 8:2 FTUCA then undergoes another attack by water at the β-carbon, resulting in the loss of the second fluorine substituent via Michael addition/elimination leading to the formation of a carbonyl. We propose a reaction sequence similar to the above transformation for the conversion of F5-hexanoate to 6,6,6-trifluoro-3-oxohexanoate(Figure 6).[41] Characterizing these defluorinating enzyme systems should be a priority goal, as it could advance understanding of the mechanisms and pathways transforming polyfluoroalkyl substances.

^{19}F NMR Demonstrates Utility for Tracing Fluorinated Catabolites. Fluorine is a monoisotopic element and has a high magnetogyric ratio with a large chemical shift range of δ > 350 ppm, resulting in well separated resonances of individual fluorine nuclei in a polyfluorinated compound.[43,44] The nuclear spin quantum number of fluorine is 1/2, and thus fluorine can couple to proximate protons and carbon atoms in characteristic manners that allow for extensive structure elucidation.[45] Terminal $-CF_3$ groups of *n*-alkanes generally absorb near δ −68 ppm on ^{19}F NMR.[46] Fluorinated carboxylic group derivatives generally have little difference in chemical shift, and detection occurs between δ −63 to −76 ppm.[46] Such chemical properties explain the proximity of the F3-hexanoate standard (δ −66.8 ppm, triplet) and the detected trifluorinated metabolite (presumably 6,6,6-trifluoro-3-oxohexanoate) (δ −66.9 ppm, triplet) NMR signals. The ^{19}F NMR experiments conducted in this study also corroborate the utility of this spectroscopic technique for absolute quantification of inorganic fluoride, as well as the identification of polyfluorinated metabolites.[47]

Polyfluorinated Catabolites Enter Fatty Acid Biosynthesis. Incorporation of organofluorine into the lipidome has been demonstrated in strain 273 cells grown with 1-fluorodecane or 1,10-difluorodecane.[18] Here, we show that organofluorine metabolites with poly- and perfluorinated carbons can also be channeled into phospholipid biosynthesis and the lipidome. Lipidomic profiling determined that the relative abundance of fluorinated lipids decreases as the degree of fluorination of the growth substrates increases from F2-decane (46.1%) → F3-decane (12.8%) → F5-decane (3.70%). These decreasing relative abundances of fluorinated glycerophospholipids suggest a shift in fluorinated glycerophospholipid incorporation into the membrane bilayer with respect to the degree of fluorination on the growth substrate. A prior study with *Pseudomonas* sp. strain 273 grown with 1,10-difluorodecane found that up to 82% of the total detected glycerophospholipids carry a single fluorine substitution in one or both sn1/sn2 acyl chains. The experimental work described herein demonstrates that the degree of fluorination on the initial substrate impacts the synthesis of long-chain fluorinated fatty acids. Assuming

https://doi.org/10.1021/acs.est.5c06771
Environ. Sci. Technol. 2025, 59, 22663−22675

fluorinated fatty acid synthesis proceeds through fluoroacetyl-acyl carrier proteins, it is possible that monofluoroacetyl-CoA is converted with higher efficiency than di- and trifluoroacetyl-CoAs (i.e., di- and trifluoroacetyl-CoAs are inferior substrates for fatty acid biosynthesis compared to monofluoroacetyl-CoA). A recent study found that bacteria may possess CoA ligases with higher affinity to fluorinated fatty acids (e.g., 1:5, 2:4, and 3:3 FTCAs) than to the nonfluorinated counterparts.[48] It is currently unclear if the enzymes involved in de novo fatty acid biosynthesis prefer the fluorinated versus nonfluorinated substrates, warranting kinetic studies to reveal if organofluorine incorporation into glycerophospholipids is due to enzyme promiscuity or involves enzymes with higher affinity to short-chains fluorinated than nonfluorinated fatty acids.

Pathways Leading to the Formation of Pentafluorinated Acyl Chains. De novo fatty acid biosynthesis is an iterative process initiated with acetyl-CoA and malonyl-CoA as building blocks.[49−53] The formation of fluoroacetyl-CoAs is a plausible explanation (i.e., entry point) for fluorinated fatty acid biosynthesis, as speculated in prior studies[16,18] However, the observed formation of penta- and decafluorinated glycerophospholipids measured in strain 273 cells grown with F5-decane cannot be explained with trifluoroacetyl-CoA serving as an initial building block, due to the origin of the $-CF_2-$ group within the sn1/sn2 acyl chains of the detected glycerophospholipids. Longer-chain length acyl-CoAs, such as pentafluorohexanoyl-CoA, pentafluorooctanoyl-CoA, and pentafluorodecanoyl-CoA, may be directly shunted into fatty acid synthesis. Such a mechanism is not unprecedented, and bacteria have been reported to directly shunt β-oxidation intermediates (e.g., octanoyl-CoA) into de novo fatty acid biosynthesis.[54,55]

Percent Fluorination Alters Membrane Lipid Composition. Even though bacteria have comparatively simple membranes, they synthesize a diverse set of fatty acids with varying degrees of unsaturations that result in several glycerophospholipid classes, each with multiple species, that allow adaptation to fluctuating environmental conditions.[56,57] Many studies have investigated the metabolism of fatty acids and glycerophospholipid classes via the application of stable isotope labeling through enrichment via the substrate pool.[58−60] Historically, a single fluorine has been considered a rather innocent isostere for hydrogen due to their relatively similar sizes, but the extent to which the chemical properties of carbons bearing multiple fluorines deviate from hydrocarbons is underappreciated.[61] Further, fluorination of the termini of glycerophospholipid tails and close packing of molecules in the membrane could also force interaction among highly electronegative moieties, which could increase the fluorous effect and lead to phase separation in the membrane.[62] This effect could explain the observation that ∼46% of detected glycerophospholipids were fluorinated when grown with F2-decane while only ∼13% of detected glycerophospholipids were fluorinated when grown with F3-decane and ∼4% of detected glycerophospholipids were fluorinated when grown with F5-decane (Figures 4 and 6). Membranes with a high percentage of fluorination among the glycerophospholipids also had a higher percentage of PE (Figure 4), which was observed previously with strain 273.[15] These findings add to a growing understanding that bacteria can alter glycerophospholipid class composition in response to environmental stimuli.[63−65] Alterations in the acyl chain composition impacts membrane fluidity, and bacteria are known to adapt to a number of environmental stimuli, such as temperature,[66] and changes in acyl chain composition were detected under all growth conditions in this study (Figure 5). The global lipidome changes triggered by the incorporation of fluorinated glycerophospholipids observed in strain 273 suggest that these molecules could impact microbial community function and structure in environmental systems and have other unanticipated ecological or ecotoxicological effects. The ecological or ecotoxicological effects of such global lipidome changes (i.e., fluoromembrane formation) are unclear and warrant exploration. Future work should assess other bacteria with AlkB-2 type alkyl fluoride dehalogenases (e.g., *Pseudomonas* spp., *Fontimonas* sp.)[16,17] for their ability to catabolize terminally polyfluorinated decanes and whether the asymmetric distribution of organofluorine incorporation into glycerophospholipid classes is a shared feature.

Implications for the Study of PFAS Biotransformation. Work presented herein demonstrates that polyfluoroalkyl substances with nonfluorinated α-, β-, and γ-carbons (or more) are susceptible to partial β-oxidation, which can support bacterial growth. Polyfluorinated fatty acids undergo β-oxidation and δ carbon defluorination (e.g., conversion of F5-hexanoate to F3-hexanaote), allowing additional cycles of β-oxidation and chain shortening. This type of reaction has been proposed in fluorotelomer biotransformation pathways,[67,68] and the identification of the enzymes involved should have a high priority for advancing mechanistic understanding and potentially developing biomarkers. Enzymes with specificity for perfluorinated $-CF_2-$ group defluorination could enable gene-, transcript-, protein, and/or metabolite-centric approaches to probe PFAS-contaminated environments for defluorination, a useful measure to document natural attenuation potential and to potentially aid environmental risk assessment. The observation that *Pseudomonas* sp. strain 273 metabolizes terminally polyfluorinated decanes demonstrates that available axenic cultures are resources to derive mechanistic understanding of processes underlying biotransformation and fate of environmentally relevant PFASs.

■ ASSOCIATED CONTENT

Supporting Information

The Supporting Information is available free of charge at https://pubs.acs.org/doi/10.1021/acs.est.5c06771.

FISE analysis for averages of five replicates and controls (Table S6), quantification of inorganic fluoride using ^{19}F NMR (Table S7), GP abundances for cells grown with F2-decane, F3-decane, and F5-decane (Table S8), glycerophospholipid abundances grown with decane (Table S9), glycerophospholipid abundances of cells grown with F2-decane (Table S10), glycerophospholipid abundances of cells grown with F3-decane (Table S11), and glycerophospholipid abundances of cells grown with F5-decane (Table S12) (XLSX)

Additional information for GC-MS analysis of polyfluorinated short chain fatty acids, procedural details for Method H and Method RP, formulae and equations, nomenclature of compounds and glycerophospholipids, external standard curves for mass balance analysis at time of inoculation (Figure S1), external standard curves for mass balance analysis following incubation (Figure S2), standards for ^{19}F NMR (Figure S3), abiotic controls for ^{19}F NMR (Figure S4), standard curve for inorganic fluoride analysis (Figure 5), fluoride release in live cultures and control incubations (Figure S6), volatility

https://doi.org/10.1021/acs.est.5c06771
Environ. Sci. Technol. 2025, 59, 22663−22675

data regarding F5-decane (Figure S7), GC-HRMS headspace analysis of F5-decane (Figure S8), relative pool size changes of glycerophospholipid classes (Figure S9), mass balance analysis for cells grown with F2-decane (Table S1), mass balance analysis for cells grown with F3-decane (Table S2), mass balance analysis for cells grown with F5-decane (Table S3), mass balance analysis for cells grown with F5-decane + decanoate (Table S4), cell enumeration through qPCR (Table S5), and full ^{19}F NMR spectra (Figures SA1−SA26) (PDF)

AUTHOR INFORMATION

Corresponding Authors

Frank E. Löffler − *Department of Civil and Environmental Engineering, Department of Biochemistry & Cellular and Molecular Biology, and Department of Biosystems Engineering and Soil Science, University of Tennessee, Knoxville, Knoxville, Tennessee 37996, United States;* orcid.org/0000-0002-9797-4279; Email: frank.loeffler@utk.edu

Shawn R. Campagna − *Department of Chemistry, University of Tennessee, Knoxville, Knoxville, Tennessee 37996, United States; Biological Small Molecule Mass Spectrometry Core, University of Tennessee, Knoxville, Knoxville, Tennessee 37996, United States;* orcid.org/0000-0001-6809-3862; Email: campagna@utk.edu

Authors

Alexander S. Walls − *Department of Chemistry, University of Tennessee, Knoxville, Knoxville, Tennessee 37996, United States*

Gao Chen − *Department of Civil and Environmental Engineering, University of Tennessee, Knoxville, Knoxville, Tennessee 37996, United States;* orcid.org/0000-0002-8767-3130

Diana Ramirez − *Department of Microbiology, University of Tennessee, Knoxville, Knoxville, Tennessee 37996, United States*

Yongchao Xie − *State Key Laboratory of Pollution Control and Resource Reuse, School of Environment, Nanjing University, Nanjing, Jiangsu 210023, China*

Broquell M. Wong − *Department of Biochemistry & Cellular and Molecular Biology, University of Tennessee, Knoxville, Knoxville, Tennessee 37996, United States*

Amanda L. May − *Center for Renewable Carbon, University of Tennessee, Knoxville, Knoxville, Tennessee 37996, United States*

Anita Thapalia − *ExxonMobil Environmental and Property Solutions Company, Spring, Texas 77389, United States*

Complete contact information is available at: https://pubs.acs.org/10.1021/acs.est.5c06771

Notes

The authors declare no competing financial interest.

ACKNOWLEDGMENTS

This work was supported by the Department of Defense, Strategic Environmental Research and Development Program (SERDP Project ER23-3601). The authors thank Dr. Katarina Jones for feedback on mass spectrometry data analysis and Dr. Carlos Steren for thoughtful guidance on ^{19}F NMR spectroscopy.

REFERENCES

(1) Krafft, M. P.; Riess, J. G. Per-and polyfluorinated substances (PFASs): environmental challenges. *COCIS* **2015**, *20* (3), 192−212.

(2) Lim, X. Tainted water: the scientists tracing thousands of fluorinated chemicals in our environment. *Nature* **2019**, *566* (7742), 26−29.

(3) Kurwadkar, S.; Dane, J.; Kanel, S. R.; Nadagouda, M. N.; Cawdrey, R. W.; Ambade, B.; Struckhoff, G. C.; Wilkin, R. Per- and polyfluoroalkyl substances in water and wastewater: a critical review of their global occurrence and distribution. *Sci. Total Environ.* **2022**, *809*, 151003.

(4) Panieri, E.; Baralic, K.; Djukic-Cosic, D.; Buha Djordjevic, A.; Saso, L. PFAS Molecules: a major concern for the human health and the environment. *Toxics* **2022**, *10* (2), 44−99.

(5) De Silva, A. O.; Armitage, J. M.; Bruton, T. A.; Dassuncao, C.; Heiger-Bernays, W.; Hu, X. C.; Karrman, A.; Kelly, B.; Ng, C.; Robuck, A.; Sun, M.; Webster, T. F.; Sunderland, E.M. PFAS exposure pathways for humans and wildlife: a synthesis of current knowledge and key gaps in understanding. *Environ. Toxicol. Chem.* **2020**, *40* (3), 631−657.

(6) Wackett, L. P. Strategies for the biodegradation of polyfluorinated compounds. *Microorganisms* **2022**, *10* (8), 1664.

(7) Wang, Y.; Liu, A. Carbon-fluorine bond cleavage mediated by metalloenzymes. *Chem. Soc. Rev.* **2020**, *49* (14), 4906−4925.

(8) Stockbridge, R. B.; Wackett, L. P. The link between ancient microbial fluoride resistance mechanisms and bioengineering organofluorine degradation or synthesis. *Nat. Commun.* **2024**, *15* (1), 4593−4605.

(9) Liu, J.; Mejia Avendano, S. Microbial degradation of polyfluoroalkyl chemicals in the environment: a review. *Environ. Int.* **2013**, *61*, 98−114.

(10) Alexandrino, D. A. M.; Mucha, A. P.; Almeida, C. M. R.; Carvalho, M. F. Atlas of the microbial degradation of fluorinated pesticides. *Crit Rev. Biotechnol* **2022**, *42* (7), 991−1009.

(11) Kumar, R.; Dada, T. K.; Whelan, A.; Cannon, P.; Sheehan, M.; Reeves, L.; Antunes, E. Microbial and thermal treatment techniques for degradation of PFAS in biosolids: A focus on degradation mechanisms and pathways. *J. Hazard Mater.* **2023**, *452*, 131212−131229.

(12) Yu, Y.; Zhang, K.; Li, Z.; Ren, C.; Chen, J.; Lin, Y. H.; Liu, J.; Men, Y. Microbial cleavage of C-F bonds in two C_6 per- and polyfluorinated compounds via reductive defluorination. *Environ. Sci. Technol.* **2020**, *54* (22), 14393−14402.

(13) Carvalho, M. F.; Oliveira, R. S. Natural production of fluorinated compounds and biotechnological prospects of the fluorinase enzyme. *Crit Rev. Biotechnol* **2017**, *37* (7), 880−897.

(14) Han, J.; Kiss, L.; Mei, H.; Remete, A. M.; Ponikvar-Svet, M.; Sedgwick, D. M.; Roman, R.; Fustero, S.; Moriwaki, H.; Soloshonok, V. A. Chemical aspects of human and environmental overload with fluorine. *Chem. Rev.* **2021**, *121* (8), 4678−4742.

(15) Xie, Y.; Chen, G.; May, A. L.; Yan, J.; Brown, L. P.; Powers, J. B.; Campagna, S. R.; Löffler, F. E. *Pseudomonas* sp. strain 273 degrades fluorinated alkanes. *Environ. Sci. Technol.* **2020**, *54* (23), 14994−15003.

(16) Xie, Y.; Ramirez, D.; Chen, G.; He, G.; Sun, Y.; Murdoch, F. K.; Löffler, F. E. Genome-wide expression analysis unravels fluoroalkane metabolism in *Pseudomonas* sp. strain 273. *Environ. Sci. Technol.* **2023**, *57* (42), 15925−15935.

(17) Hendricks, L.; Reinhardt, C. R.; Green, T.; Kunczynski, L.; Roberts, A. J.; Miller, N.; Rafalin, N.; Kulik, H. J.; Groves, J. T.; Austin, R. N. *Fontimonas thermophila* Alkane Monooxygenase (FtAlkB) Is an Alkyl Fluoride Dehalogenase. *J. Am. Chem. Soc.* **2025**, *147*, 9085−9090.

(18) Xie, Y.; May, A. L.; Chen, G.; Brown, L. P.; Powers, J. B.; Tague, E. D.; Campagna, S. R.; Löffler, F. E. *Pseudomonas* sp. strain 273 incorporates organofluorine into the lipid bilayer during growth with fluorinated alkanes. *Environ. Sci. Technol.* **2022**, *56* (12), 8155−8166.

(19) Kumar, S. P. J.; Prasad, S. R.; Banerjee, R.; Agarwal, D. K.; Kulkarni, K. S.; Ramesh, K. V. Green solvents and technologies for oil extraction from oilseeds. *Chem. Cent J.* **2017**, *11*, 1−9.

(20) Zheng, X.; Qiu, Y.; Zhong, W.; Baxter, S.; Su, M.; Li, Q.; Xie, G.; Ore, B. M.; Qiao, S.; Spencer, M. D.; Zeisel, S. H.; Zhou, Z.; Zhao, A.;

Jia, W. A targeted metabolomic protocol for short-chain fatty acids and branched-chain amino acids. *Metabolomics* **2013**, *9* (4), 818−827.
(21) Wuthrich, C.; Fan, Z.; Vergeres, G.; Wahl, F.; Zenobi, R.; Giannoukos, S. Analysis of volatile short-chain fatty acids in the gas phase using secondary electrospray ionization coupled to mass spectrometry. *Anal Methods* **2023**, *15* (5), 553−561.
(22) Garcia-Villalba, R.; Gimenez-Bastida, J. A.; Garcia-Conesa, M. T.; Tomas-Barberan, F. A.; Carlos Espin, J.; Larrosa, M. Alternative method for gas chromatography-mass spectrometry analysis of short-chain fatty acids in faecal samples. *J. Sep Sci.* **2012**, *35* (15), 1906−1913.
(23) Ritalahti, K. M.; Amos, B. K.; Sung, Y.; Wu, Q.; Koenigsberg, S. S.; Löffler, F. E. Quantitative PCR targeting 16S rRNA and reductive dehalogenase genes simultaneously monitors multiple *Dehalococcoides* strains. *Appl. Environ. Microbiol.* **2006**, *72* (4), 2765−2774.
(24) Xie, Y.; Chen, G.; Ramirez, D.; Yan, J.; Löffler, F. E. Complete Genome Sequence of *Pseudomonas* sp. Strain 273, a Haloalkane-Degrading Bacterium. *Microbiol Resour Announc* **2023**, *12* (7), No. e0017623.
(25) Buszewski, B.; Noga, S. Hydrophilic interaction liquid chromatography (HILIC)-a powerful separation technique. *Anal Bioanal Chem.* **2012**, *402* (1), 231−247.
(26) Mal, M.; Wong, S. A HILIC-based UPLC-MS method for the separation of lipid classes from plasma. *Waters Application Note*; 720004048en; 2011; pp 1−9.
(27) Woodall, B. M.; Harp, J. R.; Brewer, W. T.; Tague, E. D.; Campagna, S. R.; Fozo, E. M. *Enterococcus faecalis* readily adapts membrane phospholipid composition to environmental and genetic perturbation. *Front Microbiol* **2021**, *12*, 1−17.
(28) Murphy, R. C.; Axelsen, P. H. Mass spectrometric analysis of long-chain lipids. *Mass Spectrom Rev.* **2011**, *30* (4), 579−599.
(29) Yang, J.; Huang, Y.; Wang, Y.; Chen, J.; Yu, M. Isobaric vapor-liquid equilibrium for binary systems of n-butyric acid with water, isopropyl acetate, n-propyl acetate, and n-methylpyrrolidone. *JCED* **2023**, *68* (8), 2037−2044.
(30) Woolf, A. A. Relative boiling points of fluoro-ethers, fluoro-amines and other fluorocarbon derivatives to fluorocarbons. *J. Fluor. Chem.* **1999**, *94* (1), 47−50.
(31) Fromel, T.; Knepper, T. P. Biodegradation of fluorinated alkyl substances. *Rev. Environ. Contam Toxicol* **2010**, *208*, 161−177.
(32) LaFond, J. A.; Hatzinger, P. B.; Guelfo, J. L.; Millerick, K.; Jackson, W. A. Bacterial transformation of per- and poly-fluoroalkyl substances: a review for the field of bioremediation. *Env. sci., Adv.* **2023**, *2* (2), 1019−1041.
(33) Parsons, J. R.; Saez, M.; Dolfing, J.; de Voogt, P. Biodegradation of perfluorinated compounds. *Rev. Environ. Contam Toxicol* **2008**, *196*, 53−71.
(34) Wackett, L. P. Nothing lasts forever: understanding microbial biodegradation of polyfluorinated compounds and perfluorinated alkyl substances. *Microb Biotechnol* **2022**, *15* (3), 773−792.
(35) Liu, J.; Lee, L. S.; Nies, L. F.; Nakatsu, C. H.; Turco, R. F. Biotransformation of 8:2 fluorotelomer alcohol in soil and by soil bacteria isolates. *Environ. Sci. Technol.* **2007**, *41* (23), 8024−8030.
(36) Tseng, N.; Wang, N.; Szostek, B.; Mahendra, S. Biotransformation of 6:2 fluorotelomer alcohol (6:2 FTOH) by a wood-rotting fungus. *Environ. Sci. Technol.* **2014**, *48* (7), 4012−4020.
(37) Hagen, D. F.; Belisle, J.; Johnson, J. D.; Venkateswarlu, P. Characterization of fluorinated metabolites by a gas chromatographic-helium microwave plasma detector-the biotransformation of 1H, 1H, 2H, 2H-perfluorodecanol to perfluorooctanoate. *Anal. Biochem.* **1981**, *118* (2), 336−343.
(38) Che, S.; Jin, B.; Liu, Z.; Yu, Y.; Liu, J.; Men, Y. Structure-specific aerobic defluorination of short-chain fluorinated carboxylic acids by activated sludge communities. *Environ. Sci. Technol. Lett.* **2021**, *8* (8), 668−674.
(39) Kim, M. H.; Wang, N.; McDonald, T.; Chu, K. H. Biodefluorination and biotransformation of fluorotelomer alcohols by two alkane-degrading *Pseudomonas* strains. *Biotechnol. Bioeng.* **2012**, *109* (12), 3041−3048.
(40) Yan, P. F.; Dong, S.; Manz, K. E.; Liu, C.; Woodcock, M. J.; Mezzari, M. P.; Abriola, L. M.; Pennell, K. D.; Capiro, N. L. Biotransformation of 8:2 fluorotelomer alcohol in soil from aqueous film-forming foams (AFFFs)-impacted sites under nitrate-, sulfate-, and iron-reducing conditions. *Environ. Sci. Technol.* **2022**, *56* (19), 13728−13739.
(41) Dinglasan, M. J.; Ye, Y.; Edwards, E. A.; Mabury, S. A. Fluorotelomer alcohol biodegradation yields poly- and perfluorinated acids. *Environ. Sci. Technol.* **2004**, *38* (10), 2857−2864.
(42) Butt, C. M.; Muir, D. C.; Mabury, S. A. Biotransformation pathways of fluorotelomer-based polyfluoroalkyl substances: a review. *Environ. Toxicol. Chem.* **2013**, *33* (2), 243−267.
(43) Ando, R.; Scheler, K.; Grant, D. M. Fluorine-19 NMR of solids containing both fluorine and hydrogen. *Prog. Nucl. Magn. Reson. Spectrosc.* **2002**, *9*, 531−550.
(44) Gerig, J. T. Fluorine NMR of Proteins. *Prog. Nucl. Magn. Reson. Spectrosc.* **1994**, *26*, 293−370.
(45) Kitevski-LeBlanc, J. L.; Prosser, R. S. Current applications of ^{19}F NMR to studies of protein structure and dynamics. *Prog. Nucl. Magn. Reson. Spectrosc.* **2012**, *62*, 1−33.
(46) Dolbier, W. *Guide to fluorine NMR for chemists*; Wiley, 2016.
(47) Kim, J.; Leonard, S. W.; Van Meter, M. I.; Kim-Fu, M. L.; Cao, D.; Field, J. A.; Chu, K. H. Nexus of soil microbiomes, genes, classes of carbon substrates, and biotransformation of fluorotelomer-based precursors. *Environ. Sci. Technol.* **2024**, *58* (46), 20553−20565.
(48) Mothersole, R. G.; Mothersole, M. K.; Goddard, H. G.; Liu, J.; Van Hamme, J. D. Enzyme catalyzed formation of CoA adducts of fluorinated hexanoic acid analogues using a long-chain acyl-CoA synthetase from *Gordonia* sp. strain NB4−1Y. *Biochem.* **2024**, *63* (17), 2153−2165.
(49) Heil, C. S.; Wehrheim, S. S.; Paithankar, K. S.; Grininger, M. Fatty Acid Biosynthesis: chain-length regulation and control. *Chembiochem* **2019**, *20* (18), 2298−2321.
(50) Parsons, J. B.; Rock, C. O. Is bacterial fatty acid synthesis a valid target for antibacterial drug discovery? *Curr. Opin Microbiol* **2011**, *14* (5), 544−549.
(51) Zhang, Y. M.; Rock, C. O. Transcriptional regulation in bacterial membrane lipid synthesis. *J. Lipid Res.* **2009**, *50* (Suppl), S115−S119.
(52) Wakil, S. J.; Stoops, J. K.; Joshi, V. C. Fatty acid synthesis and its regulation. *Annu. Rev. Biochem.* **1983**, *52*, 537−579.
(53) Zhang, Y. M.; Rock, C. O. Membrane lipid homeostasis in bacteria. *Nat. Rev. Microbiol* **2008**, *6* (3), 222−233.
(54) Yuan, Y.; Leeds, J. A.; Meredith, T. C. *Pseudomonas aeruginosa* directly shunts β-oxidation degradation intermediates into de novo fatty acid biosynthesis. *J. Bacteriol.* **2012**, *194* (19), 5185−5196.
(55) Yao, J.; Rock, C. O. Exogenous fatty acid metabolism in bacteria. *Biochimie* **2017**, *141*, 30−39.
(56) Appala, K.; Bimpeh, K.; Freeman, C.; Hines, K. M. Recent applications of mass spectrometry in bacterial lipidomics. *Anal Bioanal Chem.* **2020**, *412* (24), 5935−5943.
(57) Jeucken, A.; Zhou, M.; Wosten, M.; Brouwers, J. F. Control of n-butanol induced lipidome adaptations in *E. coli*. *Metabolites* **2021**, *11* (5), 286−300.
(58) Bleijerveld, O. B.; Houweling, M.; Thomas, M. J.; Cui, Z. Metabolipidomics: profiling metabolism of glycerophospholipid species by stable isotopic precursors and tandem mass spectrometry. *Anal. Biochem.* **2006**, *352* (1), 1−14.
(59) Ecker, J.; Liebisch, G. Application of stable isotopes to investigate the metabolism of fatty acids, glycerophospholipid and sphingolipid species. *Prog. Lipid Res.* **2014**, *54*, 14−31.
(60) Woodall, B.; Fozo, E. M.; Campagna, S. R. Dual stable isotopes enhance lipidomic studies in bacterial model organism *Enterococcus faecalis*. *Anal Bioanal Chem.* **2023**, *415* (17), 3593−3605.
(61) Meanwell, N. A. Fluorine and fluorinated motifs in the design and application of bioisosteres for drug design. *J. Med. Chem.* **2018**, *61* (14), 5822−5880.
(62) Cametti, M.; Crousse, B.; Metrangolo, P.; Milani, R.; Resnati, G. The fluorous effect in biomolecular applications. *Chem. Soc. Rev.* **2012**, *41* (1), 31−42.

https://doi.org/10.1021/acs.est.5c06771
Environ. Sci. Technol. 2025, 59, 22663−22675

(63) Basso, J. T. R.; Jones, K. A.; Jacobs, K. R.; Christopher, C. J.; Fielland, H. B.; Campagna, S. R.; Buchan, A. Growth substrate and prophage induction collectively influence metabolite and lipid profiles in a marine bacterium. *mSystems* **2022**, *7* (5), No. e0058522.
(64) Riviere, A.; Selak, M.; Lantin, D.; Leroy, F.; De Vuyst, L. *Bifidobacteria* and butyrate-producing colon bacteria: importance and strategies for their stimulation in the human gut. *Front Microbiol* **2016**, *7*, 979.
(65) Willdigg, J. R.; Helmann, J. D. Mini review: bacterial membrane composition and Its modulation in response to stress. *Front Mol. Biosci* **2021**, *8*, 634438.
(66) Holm, H. C.; Fredricks, H. F.; Bent, S. M.; Lowenstein, D. P.; Ossolinski, J. E.; Becker, K. W.; Johnson, W. M.; Schrage, K.; Van Mooy, B. A. S. Global ocean lipidomes show a universal relationship between temperature and lipid unsaturation. *Science* **2022**, *376* (6600), 1487−1491.
(67) Wang, N.; Liu, J.; Buck, R. C.; Korzeniowski, S. H.; Wolstenholme, B. W.; Folsom, P. W.; Sulecki, L. M. 6:2 fluorotelomer sulfonate aerobic biotransformation in activated sludge of waste water treatment plants. *Chemosphere* **2011**, *82* (6), 853−858.
(68) Berhanu, A.; Mutanda, I.; Taolin, J.; Qaria, M. A.; Yang, B.; Zhu, D. A review of microbial degradation of per- and polyfluoroalkyl substances (PFAS): biotransformation routes and enzymes. *Sci. Total Environ.* **2023**, *859*, 160010−160025.

https://doi.org/10.1021/acs.est.5c06771
Environ. Sci. Technol. 2025, 59, 22663−22675